symmetry during the process of the adsorption, (ii) the influence of sulfonic groups is minimal or negligible on the overall behavior of Pc molecules, and (iii) the TsPc molecules adsorbed on the silver electrode are adsorbed mainly through the phys- rather than chem-adsorption mechanism. In addition, use of the incident laser polarization information and the recorded polarized and depolarized Raman spectra from adsorbed TsPc on a silver electrode suggests an edge-on molecular orientation.

The laser excitation in the adsorption Q bands provides resonant SERS but at the same time indicates photoeffects. Nonresonant laser excitation of the adsorbed TsPc appears more suitable for studying electrochemical processes and provides very specific answers in the case of adsorbed monolayers on the electrode interfaces.

Raman ORC's obtained by using SERS simultaneously with cyclic voltammetry allow detailed analysis of the oxidation-reduction process in TsPc. Such studies have a significant bearing on the analysis of the oxidation of TsPc and most probably of the behavior of heme molecules in the presence of oxygen molecules. The Raman ORC's reported here indicate that pyrrole ring electrons are delocalized and that Raman ORC's can provide assignment of the cyclic voltammogram peaks.

The experimental data presented also show a direct correlation between the Raman scattering effect and an electrochemical process; this may prove to be a very powerful analytical methodology.

Acknowledgment. We thank DOE for partial support of this work, and B. S.-G. thanks Dr, D. Schuele and S. S. for financial help.

Registry No. H_2-TSPc, 19497-02-0; Co-TSPc, 29012-54-2; Fe-TSPc, 86508-34-1; Ag, 7440-22-4.

Role of Excited Atomic States in the Active Sites of Transition Metals for Oxidative and Reductive Catalytic Processes

J. García-Prieto,† M. E. Ruíz,† and O. Novaro*‡

Contribution from the Instituto Mexicano del Petróleo, Investigación Básica de Procesos, A.P. 14-805 México 07730 D.F., Mexico, and Instituto de Física, U.N.A.M., A.P. 20-364 México 01000 D.F., Mexico. *Received November 20, 1984*

Abstract: Model potential configuration-interaction calculations using a variational reference state of ~100 configurations and a Møller-Plesset perturbational study including another ~750 000 configurations are addressed in the study of a model for the oxidative and reductive processes that occur at a metallic copper catalyst. The main goal is to show the central role that is played by the excited states of a transition metal, since without their detailed knowledge, one may grossly overestimate the activation barrier for the H-H bond breaking in the chemisorption process of a H_2 molecule. The potential energy surfaces relevant to the study of the oxidative and reductive processes include those used before in the study of the photochemical reaction of a Cu atom with a H_2 molecule at matrix isolation conditions and also additional calculations for a total three-dimensional image of these important potential energy surfaces. We also study the relative minima for the intermediate CuH_2 system, which is unobservable for the photochemical process as reported elsewhere, but very crucial here as a model of the chemisorbed species of the oxidative and reductive catalytic processes. In consequence a very detailed description of the bent and linear geometries of the CuH_2 complex is given, with emphasis on the molecular orbital structures, charge transfer, etc. From all this we conclude that two possible chemisorbed forms of H_2 on copper exist: one with a very weak H-H bond, another with only atomic hydrogen on the copper sites. Our calculations predict an energy barrier for chemisorption of 28 kcal/mol, virtually identical with the experimental dissociative adsorption energy for H_2 on copper.

I. Introduction

It has now been quite some time since the first proposal[1] to correlate data on "naked" metal atoms or "naked" metal clusters with those of the actual surface of a heterogeneous catalyst was advanced. This was based on a wealth of experimental data available from a matrix isolation technique[2] and led to the very tempting idea of tailor-making reaction intermediates that ought to reproduce (or model) the actual chemical situations through a catalytic cycle. It should be mentioned that this is a different concept from the "catalyst tailoring" approach in homogeneous catalysis.[3]

About the same time, the first proposals for using ab initio studies of metal cluster complexes[4] to understand the chemistry of metal surfaces were advanced, and also many semiempirical molecular orbital studies were carried out.[5] The latter are, of course, greatly limited by their use of empirical data to really give significant and independent predictions to the catalytic phenomena. As concerns the ab initio approach, they have concentrated mostly on building large enough (nontransition) metal clusters[6] to represent reasonably well the collective electronic properties of infinite surfaces, in spite of continuous warnings, such as those of Moskovits[7] that collective phenomena do not correlate per se with molecular adsorption in the limit of small particles. We have proposed elsewhere a different way to go into the question of how collective effects can be evaluated for finite clusters.[8]

† Instituto Mexicano del Petróleo.
‡ Instituto de Física.

(1) Ozin, G. A. *Acc. Chem. Res.* **1977**, *10*, 21.
(2) (a) Ozin, G. A. *Catal. Rev.-Sci. Eng.* **1977**, *16*, 191, and references cited therein. (b) Ozin, G. A. *Coord. Chem. Rev.* **1979**, *28*, 117, and references cited therein.
(3) Olivé, S.; Henrici-Olivé, G. "Homogeneous Catalysis"; Elsevier: Zurich, 1978.
(4) (a) Schaefer, H. F. *Acc. Chem. Res.* **1977**, *10*, 287. (b) Goddard, W. A. *Chem. Eng. News* **1976**, *54*, 14.
(5) (a) Anderson, A. B.; Hoffmann, R. *J. Chem. Phys.* **1974**, *61*, 4545. (b) Schrieffer, J. R. *J. Vac. Sci. Technol.* **1976**, *13*, 335. (c) Mason, M. G.; Baetzold, R. C. *J. Chem. Phys.* **1976**, *64*, 271. (d) Blyholder, G. *Ibid.* **1975**, *62*, 3192. (e) Anderson, A. B. *Ibid.* **1976**, *65*, 1729. (f) Johnson, K. H.; Messmer, R. P. *J. Vac. Sci. Technol.* **1974**, *11*, 236.
(6) (a) Bagus, P. S.; Schaefer, H. F.; Bauschlicher, Ch. W. *J. Chem. Phys.* **1983**, *78*, 1390. (b) Bauschlicher, Ch. W.; Liskow, D. H.; Bender, C. F.; Schaefer, H. F. *Ibid.* **1975**, *62*, 4815. (c) Bauschlicher, Ch. W.; Bender, C. F.; Schaefer, H. F.; Bagus P. S. *Chem. Phys.* **1976**, *15*, 227. (d) Hermann, K.; Bagus, P. S. *Phys. Rev. B* **1978**, *17*, 4082.
(7) Moskovits, M. *Acc. Chem. Res.* **1979**, *12*, 229.

0002-7863/85/1507-5635$01.50/0 © 1985 American Chemical Society

In any case many catalytic phenomena can be related to molecular adsorption, rather than to collective "plasmon" or infinite surface behavior. This would be the case, for example, in homogeneous organometallic catalysts, highly dispersed metallic cluster catalysts with metal particles of radii of a few ångströms,[9] and again all the heterogeneous metal catalysts that have repeatedly been shown to have their active centers at the irregularities on the surface:[10] the kinks, steps, etc., where the local metal atoms are in situations quite similar to that of small naked clusters in an inert matrix, or a naked atom or cluster studied by rigorous theoretical methods.

In this sense this approach has been broadly applied to the study of the interaction of transition metal atoms, ions, and transition metal clusters with organic or inorganic fragments in order to model chemisorption states or intermediates that occur through a homogeneous or heterogeneous catalytic cycle.[1,2,4,11] An example of this is the interesting correlation between theory and experimental matrix isolation work for the $Ni_n(C_2H_4)_m$[12] and Pd–C_2H_4[13] systems, intended to model the first steps of adsorption of ethylene on nickel and palladium surfaces.

Recently, research (theoretical and experimental) of the activation of the H–H bond of the H_2 molecule by photoexcited Cu* atoms[14–16] and of the recombination reaction H + CuH → Cu + H_2[17,18] has been published. Considering that the theoretical results[15,16,18] have some relevance to the chemisorption, the oxidative addition, and the reductive elimination of H_2 on transition metal active centers of a homogeneous or heterogeneous copper catalyst (and moreover, the information may probably be valuable also for other metals), we shall in this paper discuss the SCF–CI results as they apply to the reaction pathways of ground-state copper atoms. We will also show that, without the explicit inclusion of the copper excited states in the reaction coordinate, the calculations would lead us to the wrong result of predicting an enormous activation barrier for the addition or elimination reaction of a H_2 molecule on a hypothetical active center of a copper cluster. Their inclusion, as we will see, corrects the picture to the point of predicting a heat of dissociative adsorption (28 kcal/mol) essentially equal to the experimental value for a metal copper surface.[19] The important role of the transition metal excited states naturally leads to speculations that they may present great relevance for the phenomena as the great changes that "catalytic promoters" or special groups on a metal complex can introduce for catalytic activity. This shall be our main objective in this paper.

II. Computational Method and Model

Details of the method and basis set used in this study have been given previously.[15,16] Briefly, we use the ab initio pseudopotential method of Durand and Barthelat[20] for our SCF–LCAO calculations with the pseudopotential parameters for Cu which were optimized and reported by Pélissier.[21] The convergence criterion for the SCF iteration energies was set at 10^{-6}. The reference Hartree–Fock orbitals are those of the Cu($d^{10}s^1$) state on which the configuration interaction (CI) studies were based. The electron correlation effects have been taken into account by a second-order perturbation theory using the CIPSI method.[22] This method allows a CI study that in our present case implies the diagonalization of a multiconfiguration reference state consisting of ~100 determinants. This in the CIPSI algorithm gives a reference energy which is taken as a zero-order energy in a perturbational approach which includes a much larger configurational space in the second order.[22] We shall report results of ~3/4 of a million configurations using the perturbative Møller–Plesset barycentric method.[22]

To give an estimation of the error bars in our calculations, we should mention that we optimized our Cu(3,2,5/2,2,2) contracted Gaussian set by simultaneously fitting the ^2S, ^2P, and ^2D states of copper. For the H atom a (4,2/2,2) set was used. The reproduction of the ground- to excited-state energy splitting for ^2P–^2S and ^2D–^2S was shown to be quite good in ref 15, so we expect our three-dimensional energy surfaces, the ^2S ground and the excited ^2P and ^2D for the Cu + H_2 reaction, to be equally well represented especially considering that we also obtained a very good description of the copper hydride and Cu_2 as mentioned there, as well as for Cu_3.[23]

We, however, shall base much of our interpretation on avoided crossings, as discussed in the following section. Here additional uncertainties are introduced, specifically the fact that the Herzberg–Teller couplings[24] are by their vibronic nature not quantitatively given in our Born–Oppenheimer approach to the problem. This will affect our estimation of the actual height of the energy barriers (i.e., we will know that they lie below the crossing point but not how much lower). Pearson,[25] however, estimates that the avoided crossing between two surfaces of equal symmetry is at most 10 kcal/mol, while for a Herzberg–Teller coupling he estimates that it is about one-tenth of this value.

In our attempt to correlate our data on the CuH_2 system to actual hydrogen adsorption on Cu surfaces, many approximations are of course introduced. If we wanted a comparison with H_2–copper surface potentials such as those obtained by Gelb and co-workers,[26,27] several warning notes are needed. Firstly, the level of approximation is different: Gelb and Cardillo[26] use classical trajectories and Gregory, Gelb, and Silbey[27] a rough quantum-mechanical approach, but both fit their results directly to reproduce the molecular beam data of ref 28. Also these authors study several types of adsorption sites on a surface of which only type C (which in the language of ref 6 are called "head-on sites") correlates with our results, and we should compare our data to such sites as shall be done in section IV. We shall show that our results fall well in accordance with the range of values reported in ref 27 and also with the conclusions of the original molecular beam studies.[28]

Finally we must mention that both in the above-mentioned studies[26,27] and our present one collective effects are not included. In our case this stems from considering a single metal atom, in theirs from the use of purely pairwise additive potentials. Our own proposal of how to evaluate and correct for such effects is through a multibody expansion as is discussed in full detail in ref 8.

III. Results

A. Reaction Pathways. We will mostly be concerned with theoretical aspects of thermal catalytic processes, namely, the oxidative addition and reductive elimination of H_2 on metallic copper. However, to fully understand the role that excited copper atom states may play on such processes, it is useful to take a look at the picture obtained in the study of photoexcited Cu* + H_2 → CuH + H reactions.[15,16] In ref 15, in fact, it was shown that the photoexcited state responsible for the H_2 capture was the (^2P)

(8) (a) García-Prieto, J.; Feng, W. L.; Novaro, O. *Surf. Sci.* **1984**, *147*, 555. (b) Feng, W. L.; Novaro, O.; Ruiz, M. E.; García-Prieto, J., *J. Mol. Catal.*, in press.

(9) See, for instance: Ruiz, M. E.; Novaro, O.; Ferreira, J. M.; Gómez, R. *J. Catal.* **1978**, *51*, 108, for ultradisperse catalyst. A whole number of *Surface Science* (Vol. 106, No. 1, 1981) was devoted to the Proceedings of Holland Meeting, "Small Particles and Inorganic Clusters".

(10) (a) Mutterties, E. L.; Rhodin, T. N.; Band, E.; Brucker, C. F.; Pretzer, W. R. *Chem. Rev.* **1979**, *79*, 91. (b) Benson, J. E.; Hwang, H. S.; Boudart, M. *J. Catal.* **1973**, *30*, 146. (c) Somorjai, G. A. *Adv. Catal.* **1977**, *26*, 2. (d) Sinfelt, J. H.; Lam, Y. A.; Cusumano, J. A.; Bennet, A. E. *J. Catal.* **1976**, *42*, 227.

(11) (a) Armentrout, P. B.; Beauchamp, J. L. *J. Am. Chem. Soc.* **1981**, *103*, 6624, 6628. (b) Jacobson, D. B.; Freiser, B. S. *Ibid.* **1983**, *105*, 5197. (c) Jones, R. W.; Staley, R. H. *Ibid.* **1982**, *104*, 2296. (d) Kappes, M. M.; Staley, R. H. *Ibid.* **1982**, *104*, 1813, 1819.

(12) Ozin, G. A.; Power, W. J.; Upton, T. H.; Goddard, W. A., III *J. Am. Chem. Soc.* **1978**, *100*, 4750.

(13) (a) Huber, H.; Ozin, G. A.; Power, W. J. *Inorg. Chem.* **1977**, *16*, 979. (b) García-Prieto, J.; Novaro, O. *Mol. Phys.* **1980**, *41*, 205.

(14) Ozin, G. A.; Mitchell, S. A.; García-Prieto, J. *Angew. Chem. Int. Ed. Engl.* **1982**, *21*, 380; *Angew. Chem. Suppl.* **1982**, 785.

(15) Ruiz, M. E.; García-Prieto, J.; Novaro, O. *J. Chem. Phys.* **1984**, *80*, 1529.

(16) García-Prieto, J.; Ruiz, M. E.; Poulain, E.; Ozin, G. A.; Novaro, O. *J. Chem. Phys.* **1984**, *81*, 5920.

(17) Ozin, G. A.; Garcie, C. *J. Phys. Chem.* **1984**, *88*, 643.

(18) Ruiz, M. E.; García-Prieto, J.; Poulain, E.; Ozin, G. A.; Novaro, O. *J. Phys. Chem.*, submitted for publication.

(19) Clark, A. "The Chemisorptive Bond"; Academic Press: New York, 1974; p 12.

(20) Durand, Ph.; Barthelat, J. C. *Theor. Chim. Acta* **1975**, *38*, 283.

(21) Pélissier, M. *J. Chem. Phys.* **1981**, *75*, 775; **1983**, *79*, 2099.

(22) Huron, B.; Malrieu, J. P.; Rancurel, P. *J. Chem. Phys.* **1973**, *58*, 5745.

(23) Ruiz, M. E., unpublished results.

(24) Herzberg, G. "Electronic Spectra and Electronic Structure of Polyatomic Molecules"; Van Nostrand Reinhold: New York, 1966; p 67.

(25) Pearson, P. G. *Acc. Chem. Res.* **1971**, *4*, 152. Pearson, P. G. "Symmetry Rules for Chemical Reactions"; Wiley: New York, 1976.

(26) Gelb, A.; Cardillo, M. J. *Surf. Sci.* **1978**, *75*, 199, and references therein.

(27) Gregory, A. R.; Gelb, A.; Silbey, R. *Surf. Sci.* **1978**, *74*, 497.

(28) Balooch, M.; Cardillo, M. J.; Miller, D. R.; Stickney, R. E. *Surf. Sci.* **1974**, *46*, 358.

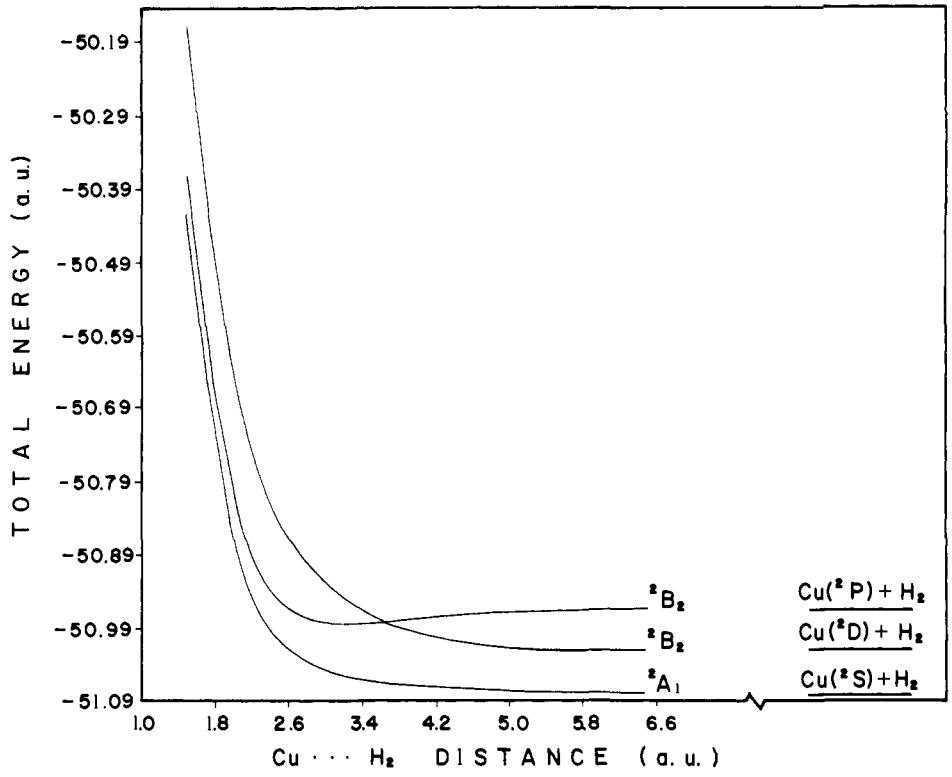

Figure 1. Total SCF energy evolution for the different Cu atom states as a function of the Cu–H_2 separation. H_2 is fixed at its equilibrium position and C_{2v} symmetry is maintained throughout.

state, explaining why in the matrix isolation experiment[14] the ground-state Cu atoms were completely inactive until bombarded by light of such frequency (~320 nm) as to induce a transition from the ground electronic state (^{2}S) to the second excited state (^{2}P) of copper

$$3d^{10}4s^1\ (^2S) \rightarrow 3d^{10}4p^1\ (^2P)$$

and at experimental conditions of 12 K[14] the cleavage of the H–H bond of the hydrogen molecule is quite efficient at the photoactivated Cu atom centers.[14,17]

The theoretical explanation is quite simple if we look at Figure 1 where the SCF curves for the side-on interactions of H_2 with Cu atoms at the ^{2}S, ^{2}P, and ^{2}D states are represented.[29] Figure 1 shows that the unrelaxed hydrogen molecule is simply repelled by the lower lying (^{2}S) ground and (^{2}D) first excited states while the higher (^{2}P) state captures it by forming a deep potential well which apparently brings the Cu(^{2}P) + H_2 curve below the Cu(^{2}D) + H_2 one at the shorter distances. Looking more carefully at the Cu–H_2 system, we see that the C_{2v} symmetry of the side-on reaction implies nine low-lying states (correlating to the $H_2(^1\Sigma_g^+)$ ground state and the Cu ^{2}S, ^{2}P, and ^{2}D states). The Cu(^{2}S) state relates with a $^2A_1$ Cu(^{2}S) + H_2 state, while the Cu(^{2}D) state gives another two $^2A_1$ states that are quite higher in energy. Also $^2B_1$, $^2A_2$, and $^2B_2$ states arise from the Cu–(^{2}D) interaction with H_2, aside from the two $^2A_1$ states previously mentioned. Three states ($^2A_1$, $^2B_1$, and $^2B_2$) arise from the Cu(^{2}P) state. The greatest attraction is by far that found for the $^2B_2$ state of Cu(^{2}P) + H_2, and this is the attractive curve represented in Figure 1. At this stage the Cu–H_2 interaction is through a classical[30] back-donation mechanism as discussed in ref 15 and schematically represented in Figure 2. The question is whether we can then assure that the photoactivation of H_2 involves only this $^2B_2$ state or not. Most other states are quite repulsive and too high in energy to really participate, but we should recall that the Cu(^{2}D)–H_2 has one state of $^2B_2$ symmetry (the lowest in energy of this type), which by the

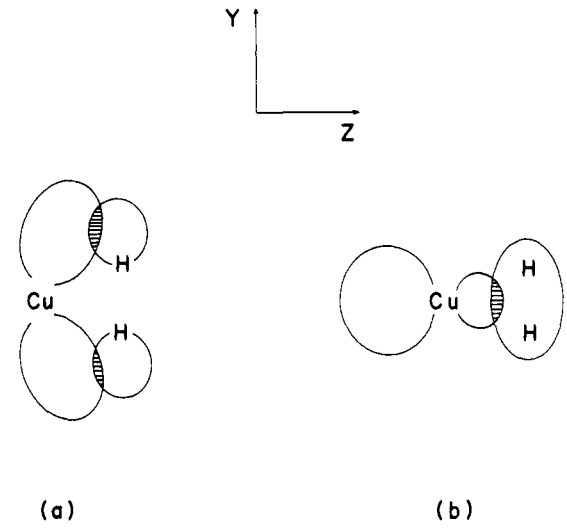

Figure 2. Schematic representation of the most relevant molecular orbitals involved in the capture of the H_2 molecule by the Cu atom at its ^{2}P state. (a) Donation from the Cu $4p_y$ orbital to the H_2 σ^* orbital. (b) Back donation from the H_2 σ orbital to the Cu s + $4p_z$ orbital.

noncrossing rule implies that the descent of the higher $^2B_2$ attractive curve (that comes from ^{2}P) would necessarily lead to an avoided crossing. In ref 16 an extensive configuration interaction (up to 750 000 configurations) led to the curves represented in Figure 3 in which also the interaction of Cu in its ground state (^{2}S) with a H_2 molecule is represented. This last potential surface has $^2A_1$ symmetry in the C_{2v} representation. In this figure we see that both $^2B_2$ curves that arise initially, one from the interaction of the (^{2}D) state with the unrelaxed molecule and the other from the similar interaction of the Cu(^{2}P) state, have attractive wells, albeit at quite different distances.

A more thorough scanning of the potential energy surfaces is necessary in order to obtain the minimal energy reaction pathways as well as the possible exit channels for the system. For this, additional CIPSI calculations have been performed for linear

(29) Preliminary results for the linear "end-on" approach has been shown to be energetically less favorable than the side-on attack (see ref 18).
(30) Chatt, J.; Duncanson, L. A. *J. Chem. Soc.* **1952**, 1953, 2939. (b) Dewar, M. J. S. *Bull. Soc. Chim. Fr.* **1951**, *18c*, 79.

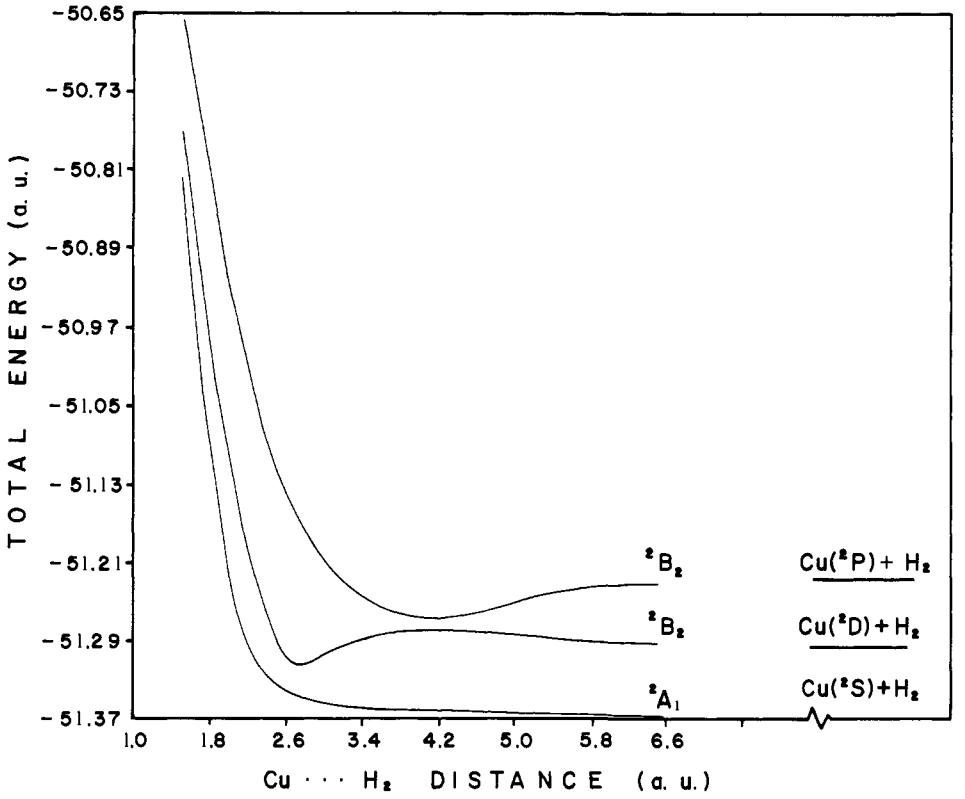

Figure 3. Total CIPSI energy evolution for the ground $^2A_1$ and the first two excited $^2B_2$ states of the CuH_2 system as a function of the Cu–H_2 distance, maintaining C_{2v} symmetry and H_2 at its equilibrium geometry. Notice the minima at both $^2B_2$ curves due to their avoided crossing not evidenced in Figure 1.

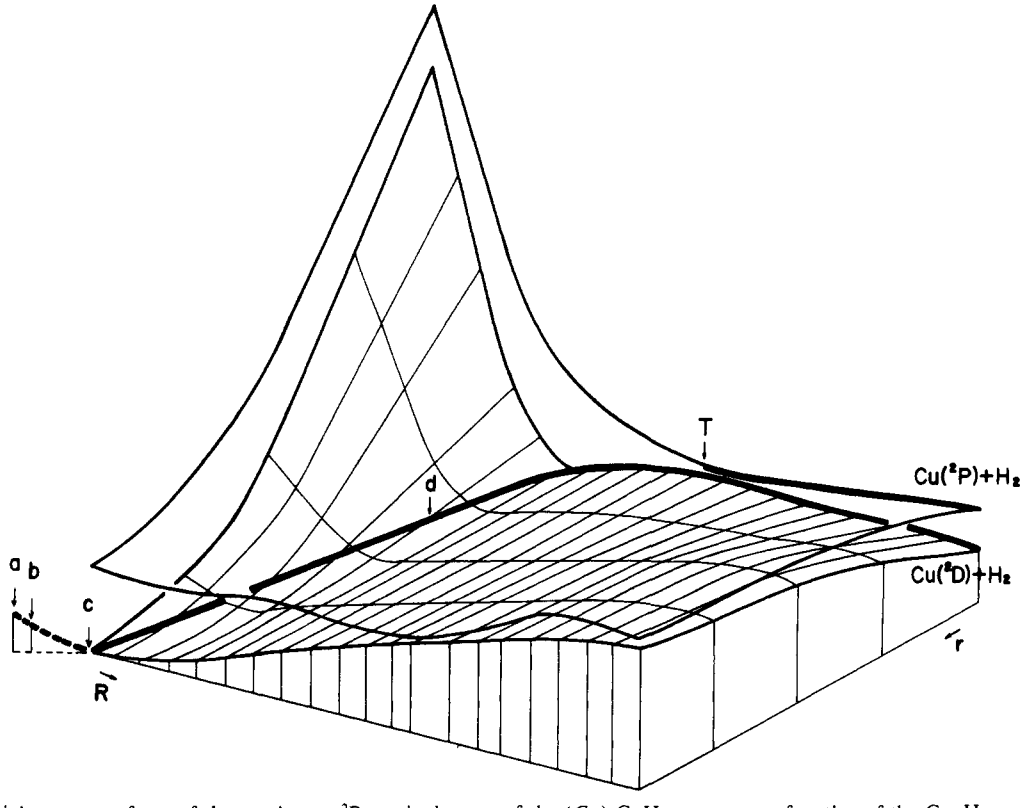

Figure 4. Potential energy surfaces of the two lowest $^2B_2$ excited states of the (C_{2v}) CuH_2 system as a function of the Cu–H_2 separation R and the internal H_2 distance r. T is the point where the nonadiabatic transition between these two surfaces occurs. For the definition of points a, b, c, and d, see text and Figure 6.

variations of the H–H bond length from r = 1.4 to 4.4 Å and of the distance from the Cu atom to the center of mass of this H_2 bond from R = 1.5 to 6.5 Å. These variations have been carried out for all the three states mentioned above (the ground $^2A_1$ and the two lowest states of $^2B_2$ symmetry). In Figure 4 the two $^2B_2$ potential energy surfaces are depicted, although for the higher state only schematically to avoid confusion. In any case, we see several points of nearest approach (even though not all of them

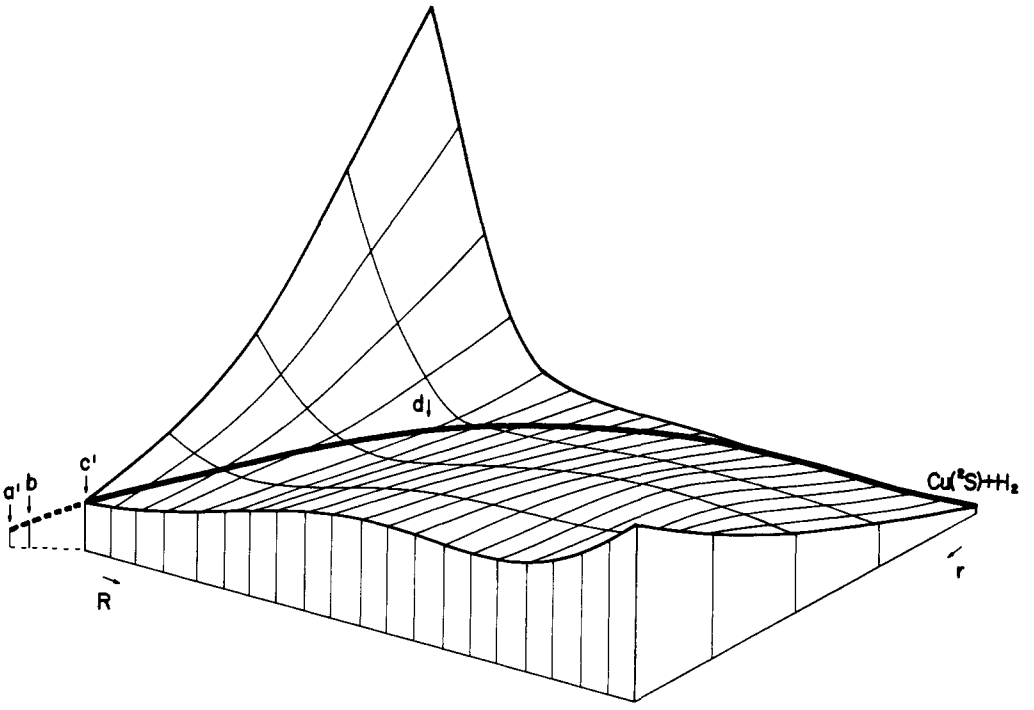

Figure 5. Potential energy surface of the $^2A_1$ ground state of the (C_{2v}) CuH_2 system as a function of R and r. The zero energy reference value is the same as in Figure 4, namely, point c which is the minimum of the lowest $^2B_2$ curve. For the definitions of points a', b, c', and d, see text and Figure 6.

are energetically accesible) showing how the avoided crossing rule applies. The optimal energy pathway for the lower $^2B_2$ curve is depicted, showing how it reaches a nearest approach to point T which in turn corresponds to the minimum of the optimal energy pathway on the upper $^2B_2$ surface. This is where the nonadiabatic transition from the upper to the lower $^2B_2$ minimal energy pathways occurs.

The lower $^2B_2$ potential energy surface has two well-defined exit channels, one toward the reactants $Cu(^2D) + H_2$ and another to point c which is the absolute minimum for this surface and consists of a bent H–Cu–H structure with a common Cu–H distance of 2.66 Å and an angle of 111.5°. Point a is the value of the energy for a linear H–Cu–H configuration, and the points b and d correspond to the crossing points between the $^2B_2$ and $^2A_1$ minimal energy pathways as shall be discussed below.

Figure 5 represents the $^2A_1$ potential energy surface, which is wholly repulsive (i.e., its minimum lies in the $Cu(^2S) + H_2$ entrance channel). Points a' and c' give the energies for the minimum and maximum of the $^2A_1$ surface (as also shown in Figure 6). The second exit channel in Figure 5 leads to another relative minimum at point a', i.e., the linear structure of state $^2A_1$ for which the common Cu–H distance is 2.84 Å.

Thus both Figures 4 and 5 present minima for the H–Cu–H system. These minima as well as a portion of the energy pathways that connect them are depicted in Figure 6, where dependence on the H–Cu–H angle instead of on r is used. In it the $^2A_1$ linear structure is shown to lie 8.6 kcal/mol above the $Cu(^2S) + H_2$ limit. The $^2B_2$ minimum is slightly closer to this limit, lying 2.6 kcal/mol below the $^2A_1$ minimum. For a thermal reaction one starts from the $Cu(^2S) + H_2$ state, and apparently to reach the minimum of the $^2A_1$ surface one would have to surmount a much too high activation barrier of 66 kcal/mol. For the matrix isolation conditions of the experiments of ref 14, however, a reasonable probability of surmounting such a barrier exists, in view of the efficient nonradiative $^2P \rightarrow {}^2S$ transition of the copper atom in the matrix[31] which could conceivably provide enough kinetic energy to the ground-state atom to surmount the barrier. Therefore, the question arises as to why even if this minimum of Figure 6 exists; the CuH_2 species was not observed in spite of careful tests using

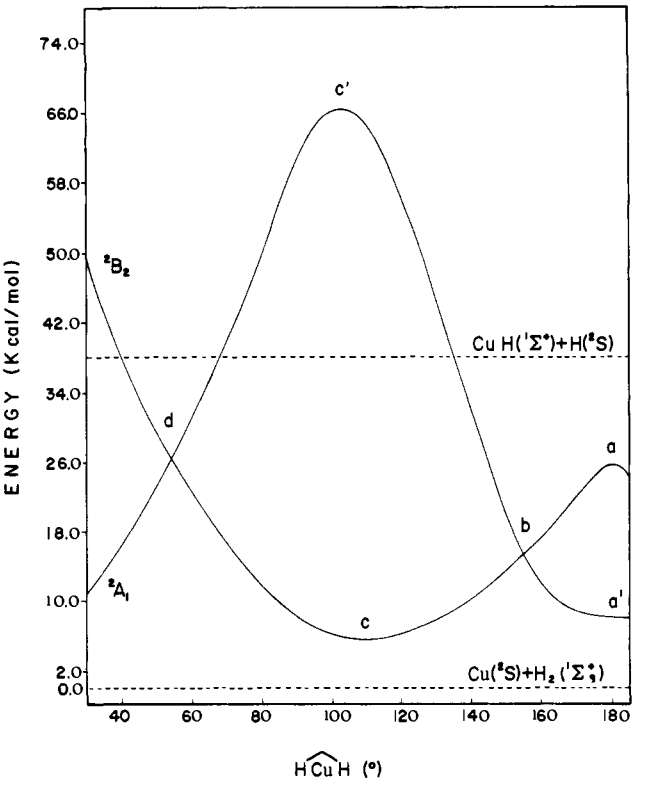

Figure 6. Angular dependence of the relative energies for the lowest $^2A_1$ and $^2B_2$ states of the CuH_2 system referred to the $Cu(^2S) + H_2$ limit. The common Cu–H distance of the C_{2v} geometry is fixed at 2.83 Å. Points c and a' are the minima of the $^2B_2$ and $^2A_1$ states, respectively, while c' and a are the maxima of the $^2A_1$ and $^2B_2$ states. The crossing points of the $^2A_1$ and $^2B_2$ surfaces are b and d.

ESR, FTIR, and UV–visible spectroscopies.[14]

The answer to this question is given in Figure 7 where the avoided crossing between the two $^2B_2$ curves is depicted as well as two other avoided crossing between the $^2B_2$ and $^2A_1$ curves. The latter repulsions substantially lower the activation barriers of the $^2A_1$ pathway. The explanation of these two extra avoided crossings

(31) Ozin, G. A.; Mitchell, S. A.; García-Prieto, J. *J. Phys. Chem.* **1982**, *86*, 473.

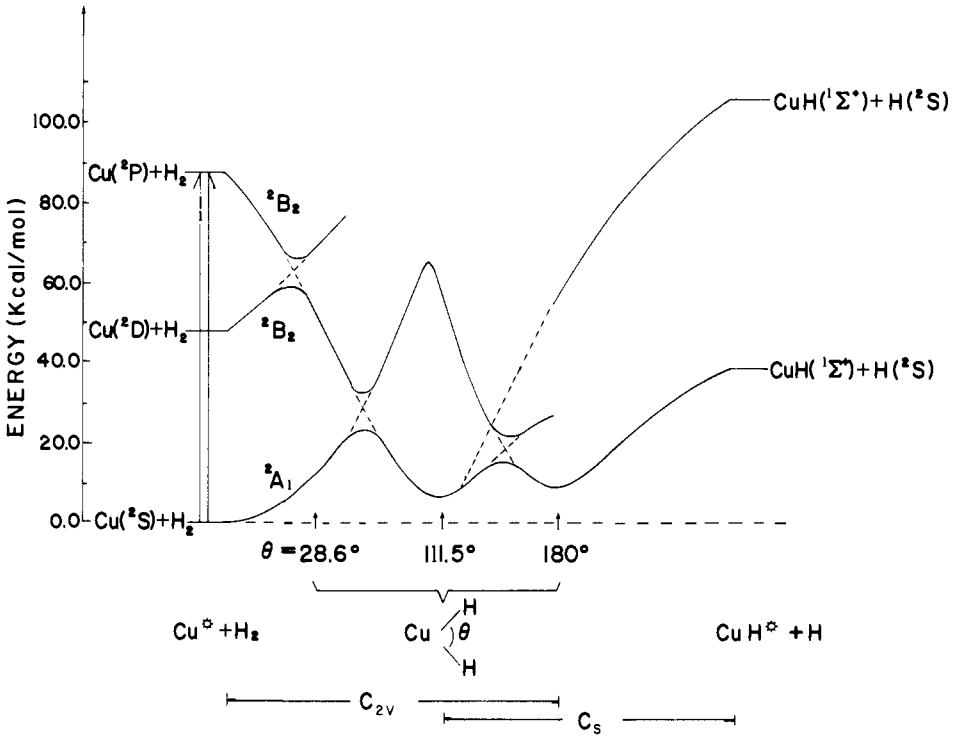

Figure 7. Exit channels for the photochemical reaction involving C_{2v} and C_s symmetries.

lies in the Herzberg–Teller theorem.[24] This theorem says that the $^2B_2$ and $^2A_1$ curves perturb each other through a vibronic coupling via the nonsymmetric stretching mode of the triatomic molecule. Such a mode is of b_2 symmetry and couples the $^2A_1$ and $^2B_2$ reaction pathways inducing the avoided crossings of Figure 7. These Herzberg–Teller curve repulsions are by their own nature not too strong and the transition probabilities consequently high. More surprisingly it was found in ref 16 that even the $^2B_2$–$^2B_2$ avoided crossing led to an uncommonly high transition probability of almost 0.5 as estimated by Landau–Zerner–Stuckelberger theory when the conditions corresponding to the experimental situation[14] are used (i.e., a kinetic energy of ~0.93 eV which comes from the energy gain from the capture of H_2 by the Cu(^{2}P) state; see Figure 3).

From Figure 7 we then have a very efficient transition process from the original $^2B_2$ interaction between the H_2 and Cu(^{2}P) to the lower lying $^2B_2$ curve and then to the $^2A_1$ curve which directly correlates to the observed products CuH + H, making Cu–H_2 a very short-lived species, thus consequently not observable. The energy increase when moving from the CuH_2 minima to the CuH($^1\Sigma_g^+$) + H(^{2}S) products is well within the energetics that the system can reach in view of the energy given to the system by the photoexcitation of the Cu atom. We should mention that the last part of Figure 7 implies the breaking of the C_{2v} symmetry as one of the hydrogen atoms leaves the linear symmetric H–Cu–H complex. If we assume this C_{2v} breaking to occur earlier (that is, before arriving to the linear configuration), the situation would be completely similar because on going from C_{2v} to C_s the $^2B_2$ and the $^2A_1$ representations will transform to $^2A'$ surfaces under C_s and therefore provoke an avoided crossing between these two surfaces of the same symmetry, which again would send us to the desired CuH + H products valley. From all of the above we can see that at the low-temperature (12 K) conditions of the experiment[14] the only way that the H_2 bond can be activated by copper atoms is by photoexcitation, and we also can understand why the intermediate complex H–Cu–H is not observed. We notice that the products can be formed not only by following the minimal energy pathway (with the high transition probabilities that eventually lead to the $^2A_1$ surface) but also by going back to the (^{2}D) or eventually to the (^{2}S) copper states. In this case, as mentioned before, the kinetic energy gained from the nonradiative transition Cu(^{2}P) → Cu(^{2}S) observed in matrix isolation conditions[31] would be enough to overcome the activation barriers, especially considering that they are now smaller. In fact, the newly formed Cu(^{2}D) would only have to overcome a barrier of some 8 kcal/mol and Cu(^{2}S) one of 28 kcal/mol as shown in Figure 7.

This last result is of great interest because we can now analyze the oxidative addition and reductive elimination of the H_2 on copper atomic centers in its ground state. These mechanisms are, in fact, involved in Figure 8 where the Herzberg–Teller coupling of the $^2A_1$ state (which arises from the interaction of the Cu atom in its ground state and the H_2 molecule) with the $^2B_2$ state brings down the high 66-kcal/mol barrier of Figure 6 to the more reasonable 28.6-kcal/mol value for the dissociative interaction of H_2. This last value is in good agreement with the well-known value of (~28 kcal/mol) for the heat of dissociative adsorption of H_2 on supported Cu metal.[19] Notice that the prediction of these small activation barriers is also in agreement with the formal symmetry rules of chemical reactions.[25] According to this theory the activation potential energy barriers can be reduced by the presence of low-lying excited states whose symmetry matches correctly those of the ground state so that the reaction can proceed.[25] In our present case the coupling of the $^2A_1$ and $^2B_2$ states by the nonsymmetrical stretching mode b_2 fulfills this condition. Figure 8 shows in more detail the reaction pathway for this process. From this figure we can also see that the reductive elimination of H_2 from the copper atomic center involves an activation energy between 20 and 22 kcal/mol which is roughly one-third of the required activation energy if the $^2B_2$ states were not present. It must be remarked that these results show that we need to consider only one copper atom in order to dissociate a H_2 molecule with a similar activation energy as observed for the metal copper surface. In this sense we can consider the copper atom as a "localized model" of an active site where the dissociative chemisorption of a H_2 molecule would occur (see below).

The dissociation of CuH_2 into CuH + H has been described before as a departure of C_{2v} symmetry. This is depicted in Figure 9 where the "tail" leading up to the CuH + H implies a steep climbing because its energy is 30 kcal/mol above the ground-state CuH_2 complex energy. Therefore under normal conditions one expects no hydrogen liberated when copper induces cleavage of the H_2 bonds. Figure 9, in fact, also given a reasonable description of the CuH + H → Cu + H_2 thermal matrix phase reaction[18]

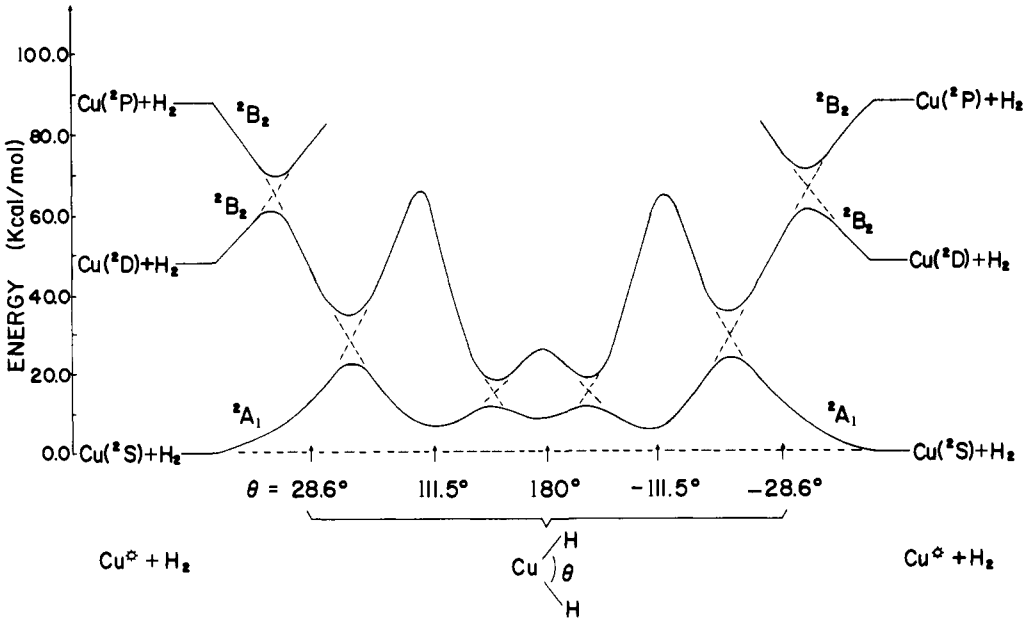

Figure 8. Physical quenching mechanism for the Cu + H_2 reaction at C_{2v} symmetry and involving the three (^{2}S, ^{2}P, and ^{2}D) states of the Cu atom.

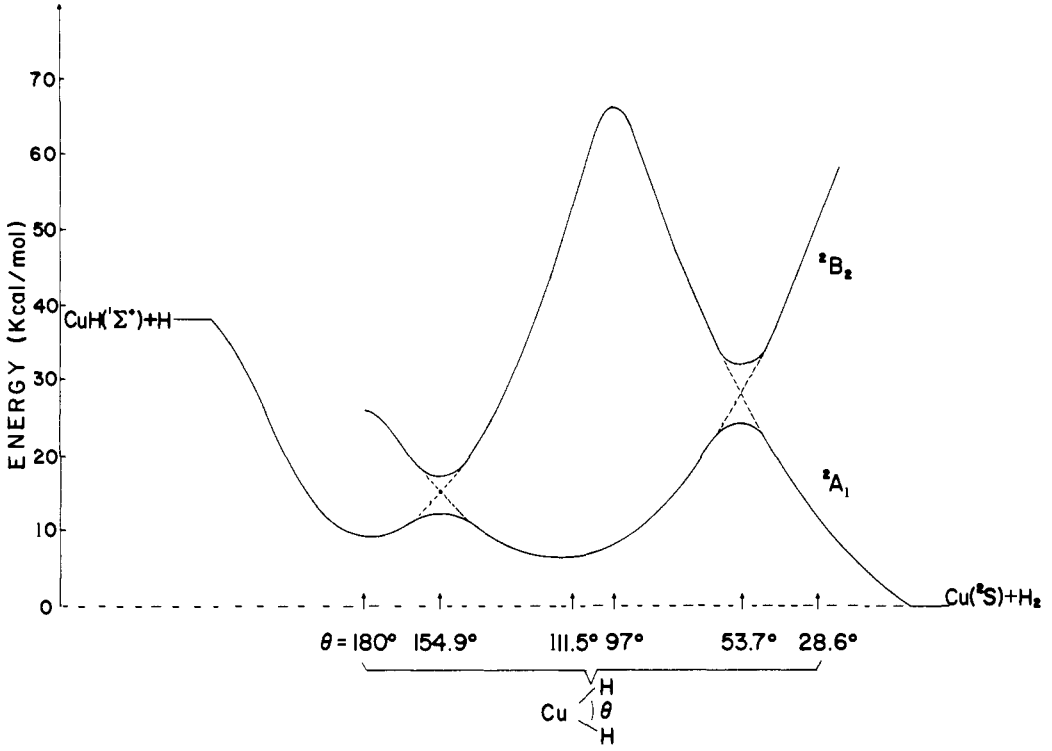

Figure 9. Adiabatic pathway for the CuH($^1\Sigma^+$) + H(^{2}S) → Cu(^{2}S) + H_2($^1\Sigma_g^+$) reaction.

for which also no evidence of a CuH_2 intermediate species was found in spite of several IR and ESR studies at 10–12 K.[17] From Figure 9 we can see that the barriers are not obstacles to the production of Cu + H_2, in agreement with experiment. The fact that the steep descendent from the CuH + H reactant valley provides large kinetic energy necessarily means that the H–Cu–H composite systems transcends its local minima and reaches the lower Cu(^{2}S) + H_2 product valley (see Figure 9).

Now we want to compare the results of similar systems.[32-40] It is interesting that the predicted activation barrier (~28 kcal/mol) for H_2 addition on a Cu atomic center is on the order of that predicted for the addition to the $Pt(Ph_3)_2$ and $Pt[P(CH_3)_3]_2$ complexes[38] (18 and 19.5 kcal/mol, respectively), and bigger than for that observed on the well-known $Ir(Cl)(CO)(PPh_3)_2$ Vaska complex (10–12 kcal/mol[36]) and on the Ni naked atomic center (~3 kcal/mol). The small value for the last case is predicted,

(32) (a) Blomberg, M.; Brandemark, U.; Petterson, L.; Siegbahn, P., *Int. J. Quantum Chem.* **1983**, *23*, 855. (b) Blomberg, M.; Siegbahn, P.; Bauschlicher, C. W. *J. Chem. Phys.* **1984**, *81*, 1373.
(33) Blomberg, M. R. A.; Siegbahn, P. *J. Chem. Phys.* **1983**, *78*, 5682.
(34) (a) Ozin, G. A.; McCaffrewy, J. G. *J. Phys. Chem.* **1984**, *88*, 645. (b) Ozin, G. A.; McCaffrewy, J. G.; McIntosh, D. F. *Pure Appl. Chem.* **1984**, *56*, 111.
(35) (a) Geoffroy, G. L.; Pierantozzi, R. *J. Am. Chem. Soc.* **1976**, *98*, 8054. (b) Geoffroy, G. L.; Bradley, M. G. *Inorg. Chem.* **1978**, *17*, 2410.
(36) Chock, P. B.; Halpern, J. *J. Am. Chem. Soc.* **1966**, *88*, 3511.
(37) Blomberg, M. R. A.; Siegbahn, P. *J. Chem. Phys.* **1983**, *78*, 986.
(38) Noell, J. O.; Hay, P. J. *J. Am. Chem. Soc.* **1982**, *104*, 4578.
(39) Balazs, A. C.; Johnson, K. H.; Whitesides, G. M. *Inorg. Chem.* **1982**, *21*, 2162.
(40) (a) Tatsumi, K.; Hoffmann, R.; Yamamoto, A.; Stille, J. K. *Bull. Chem. Soc. Jpn.* **1981**, *54*, 1857. (b) Komiya, S.; Albright, T. A.; Hoffmann, R.; Kochi, J. K. *J. Am. Chem. Soc.* **1976**, *98*, 7255; **1977**, *99*, 8440.

Table I. Equilibrium Geometries for the $^2A_1$ and $^2B_2$ States of the CuH_2 Molecule[a]

molecule	state	geometry parameter	geometry value
CuH	$^1\Sigma^+$	R(Cu-H)	2.72 Å
HCuH	$^2A_1$	R(Cu-H)	2.84 Å
		∠HCuH	180.0°
	$^2B_2$	R(Cu-H)	2.66 Å
		∠HCuH	111.5°

[a] That for CuH has been included for comparison.

however, considering that the Ni atom is at its d^9s^1 (^1D) excited state; assuming the d^8s^2 (^3F) ground state, this activation barrier increases to 48 kcal/mol,[33] which can be reduced to ~18 kcal/mol considering a spin–orbital coupling of the $^1A_1$ and $^3B_1$ potential energy surfaces (that correlate with Ni(^1D) + H^2 and Ni(^3F) + H_2 limits, respectively) at the crossing point. It has been speculated that the bent equilibrium configuration state $^1A_1$ of the NiH_2 system is probably the ground state of the metal complex when ligands are added;[33] that is, this state is probably very similar to the cis conformation of L_nNiH_2 which is involved in reductive elimination and oxidative addition of H_2 in observed reactions. In general terms, the addition reaction in all these systems seems to follow the same pattern, that is, an initial repulsion of the H_2 molecule by the metal atomic center (as a consequence of the energy barrier). As the interaction distance decreases, there appears a delocalization of the d_{yz} metal orbital into the σ^* antibonding orbital of H_2 (and the σ orbital of H_2 on the s + $d_{x^2-y^2}$ of the metal), inducing therefore a weakening of the H–H bond, the formation of the metal–hydrogen bonds, and the transfer of negative charge on the hydride ligand.

The predicted activation barrier for the H_2 elimination (20–22 kcal/mol) is, on the other hand, similar for the metal complexes mentioned before, 23 kcal/mol for *cis*-$PtH_2(Ph_3)_2$[38] and 25 kcal/mol for $H_2Ir(Cl)(CO)(PPh_3)_2$,[36] but it is larger than that for the naked NiH_2 complex[32] (~11 kcal/mol). The fact that the energy of the equilibrium configurations of CuH_2 lies above that of the Cu(^2S) + H_2 limit (less than 9 kcal/mol) would imply an instability of this complex. However, it is highly probable that the inclusion of *f* functions into the Cu basis set would bring down this energy to the point that would be below that limit. This is the case, for example, for the Ni + H_2 system where inclusion of the *f* functions into the Ni basis set increases the CCI well depth of the $^1A_1$ state by ~7 kcal/mol.[33,37] We can notice, on the other hand, that the adding of ligands would stabilize strongly this complex as observed in the other systems.[32,38]

B. Structure and Molecular Properties of the Cu–H_2 Adsorption Site. In order to know more details of the chemisorption state of a H_2 molecule on a copper metal surface, we must investigate the electronic structure and molecular properties of the CuH_2 complex, assuming that it represents a "localized model" for chemisorption of molecular hydrogen on a metal copper surface.

The relative energy and the optimized molecular geometries for the first two electronic states of the CuH_2 molecular complex, shown in Figure 7 and Table I, indicate that its electronic ground state is $^2B_2$ with a bent geometry configuration. As indicated before this state is only 2.6 kcal/mol below the $^2A_1$ state in its linear equilibrium configuration. We expect by Herzberg–Teller coupling an avoided crossing between the potential energy surfaces of both states at the 154.9 and 53.7° HCuH angular coordinates with a common 2.84 Å Cu–H distance, respectively. The first crossing is therefore a pathway for the transformation of the $^2B_2$ to $^2A_1$ electronic state, that is, the interconversion from a bent equilibrium configuration to a linear one, overcoming a small activation barrier of less than 8 kcal/mol. These two stable equilibrium configurations indicate the existence of two different kinds of adsorption on a metal copper surface. The more stable is the state were the two H atoms are linked to a Cu atom center with a H–H bond almost broken. It represents the first chemisorptive step in the dissociative chemisorption of the H_2 molecule on a copper metal surface. The second state corresponds to the truly dissociated state which would be the precursor for the formation of H atom adsorption sites. Schematically the dissociative chemisorption of a H_2 molecule on a copper metal surface would be as follows:

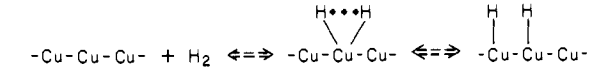

Table II. Charge Distribution Analysis for the $^2B_2$ and $^2A_1$ Electronic States of the Copper Dihydride Molecule

charge	distribution	$^2B_2$	$^2A_1$
per atom	Cu	10.804	10.360
center	H	1.098	1.320
	Cu: 3d	9.727	9.555
per atomic	Cu: 4s	0.685	0.587
orbital	Cu: 4p	0.372	0.215
	H: 1s	1.082	1.307

Table III. Computed Molecular Properties for the $^2B_2$ and $^2A_1$ Electronic States of the Copper Dihydride Molecule at Their Equilibrium Position

property	$^2B_2$	$^2A_1$
dipole moment (au)	1.018	0.000
quadrupole moment tensor (au)		
Q_{xx}	9.767	9.365
Q_{yy}	0.000	0.000
Q_{zz}	−6.689	−2.115
Q_{xy}	0.000	0.000
Q_{zz}	0.120	0.000
Q_{yz}	−6.778	9.365

Table IV. Main Contributions of the Atomic Orbitals to the Molecular Orbitals for the Bent Equilibrium Configuration

orbital	energy (au)	atomic orbital combination[a]
$1a_1$	−0.6019	$(0.6 + 0.4)d_{x^2-y^2} + (0.4 + 0.3)d_{z^2} - (0.1)s_{H_1} - (0.1)s_{H_2}$
$2a_1$	−0.5795	$(0.4 + 0.2)d_{x^2-y^2} - (0.6 + 0.4)d_{z^2} - (0.1)s_{H_1} - (0.1)s_{H_2}$
$1a_2$	−0.5790	$(0.7 + 0.5)d_{xy}$
$1b_1$	−0.5755	$(0.7 + 0.5)d_{xz}$
$1b_2$	−0.5624	$(0.6 + 0.4)d_{yz} + (0.2 + 0.1)s_{H_1} - (0.2 + 0.1)s_{H_2}$
$3a_1$	−0.4191	$(0.4 + 0.1)s + (0.3 + 0.1)d_{x^2-y^2} + (0.3 + 0.2)s_{H_1} + (0.3 + 0.2)s_{H_2}$
$2b_2$ (HOMO)	−0.1876	$-(0.1 + 0.3)p_y + (0.3 + 0.2)d_{yz} - (0.3 + 0.3)s_{H_1} + (0.3 + 0.3)s_{H_2}$
$4a_1$ (LUMO)	+0.0360	$(0.1 + 0.7)s - (0.6)p_z - (0.1 + 0.2)s_{H_1} - (0.1 + 0.2)s_{H_2}$

[a] Coefficients of the LCAO expansion are in parentheses. A double number comes from the double-ζ basis set used in the present calculations.

Table V. Main Contributions of the Atomic Orbitals to the Molecular Orbitals for the Linear Equilibrium Configuration

orbital	energy (au)	atomic orbital combination[a]
$1a_2$	−0.6647	$(0.7 + 0.5)d_{xy}$
$1b_2$	−0.6647	$(0.7 + 0.5)d_{yz}$
$1b_1$	−0.6455	$(0.7 + 0.5)d_{xz}$
$1a_1$	−0.6455	$-(0.37 + 0.23)d_{x^2-y^2} + (0.6 + 0.4)d_{z^2}$
$2a_1$	−0.6081	$-0.1s + (0.4 + 0.3)d_{x^2-y^2} + (0.3 + 0.2)d_{z^2} - (0.2 + 0.1)s_{H_1} - (0.2 + 0.1)s_{H_2}$
$2b_2$	−0.3812	$0.1p_y + (0.3 + 0.4)s_{H_1} - 0.1p_{yH_1} - (0.3 + 0.4)s_{H_2} - 0.1p_{yH_2}$
$3a_1$ (HOMO)	−0.2398	$(0.4 + 0.2)s + (0.4 + 0.2)d_{x^2-y^2} + (0.2 + 0.1)d_{z^2} + (0.1 + 0.1)s_{H_1} + (0.1 + 0.1)s_{H_2}$
$2b_1$ (LUMO)	+0.0748	$(1.0)p_z$

[a] Coefficients of the LCAO expansion are in parentheses. A double number comes from the double-ζ basis set used in the present calculations.

Some SCF molecular properties of the CuH_2 molecular complex are summarized in Tables II–V. Tables II and III show the

Mulliken charge distribution and dipole and quadrupole moments, respectively, whereas Tables IV and V summarize the main contribution of the atomic orbitals for the two equilibrium states found for this molecular complex.

From Table II we can see that there is a net charge transfer from the Cu to the hydrogen atoms, and, as expected for a copper complex in an oxidation state 2, this charge transfer increases when one reaches the linear equilibrium configuration. These results predict, therefore, a slightly ionic CuH_2 molecular complex of the $H^{\delta-}Cu^{2\delta+}H^{\delta-}$ type, with a dipole moment of 2.6 D for the bent equilibrium configuration and zero value for the symmetrically linear configuration.

The large H–H distance (4.4 Å, as can be deduced from Table I) in the bent equilibrium configuration points to a CuH_2 molecular complex with a H–H bond almost broken. The bonding between the Cu atom and the H atoms in this complex can be described, therefore, as the interaction of a $Cu^{2\delta+}$ center and two equivalent $H^{\delta-}$ ions, having also a strong covalent contribution to the Cu–H bonding.

A further analysis of the charge distribution reveals first the same tendency in the occupation numbers of the 3d, 4s, and 4p orbitals of the Cu atomic centers in both equilibrium configurations and, on the other hand, the probable participation of the three atomic orbitals in the molecular bond. A SCF molecular orbital analysis, presented in Tables IV and V, shows in fact that the simultaneous participation of those atomic orbitals are fundamental in the stabilization of this molecular species. The way in which these atomic orbitals participate in the molecular orbital formation is obviously different for each equilibrium configuration. Moreover, at the CI level it was found that very important correlation effects exist, contributing substantially to the stabilization of the CuH_2 molecular complex. These effects are basically the flexibility of the d closed shell, reducing its repulsive nature, and the relaxation of the s, p, and d orbitals along the axis of approach to the H_2 molecule.[15] This means that the participation of the d orbitals of the Cu atom is crucial in the breaking of the H_2 molecule as well as in the stabilization of the CuH_2 molecular complex (in spite of the speculations to the contrary for this metal[32,33]), and, more important, it establishes certain similarities in the mechanism of H–H bond activation with respect to other transition metals.[32,38-40]

An analysis of Tables IV and V reveals that the stabilization of the linear configuration comes mainly from the $2a_1$, $3a_1$, and $2b_2$ molecular orbitals, whereas for the bent equilibrium configuration it is from the $1a_1$, $2a_1$, $3a_1$, $1b_2$, and $2b_2$ molecular orbitals. As pointed out[39] in a similar analysis, the classification of these molecular orbitals as bonding, nonbonding, or antibonding by the sole inspection of the wave functions is not straightforward. Nevertheless, we can consider with certain confidence that the $2a_1$, $1b_2$, $3a_1$, and $2b_2$ molecular orbitals for bent equilibrium configuration contribute to the bonding whereas the $1a_1$ does not. It is interesting that similar molecular orbital bonds are found in the bonding of H_2 to bis(phosphine)platinum complexes[38,39] and on naked nickel atoms.[33] These orbitals represents mainly the delocalization of the d_{yz} metal orbital into the antibonding orbital σ^* of H_2 and that of the σ orbital of H_2 interacting with the s and $d_{x^2-y^2}$ orbitals of the metal center. For the linear configuration the $2b_2$ and $3a_1$ molecular orbitals are bonding whereas the $2a_1$ is antibonding. Once again for this last molecular configuration there are similar molecular bonds as in the NiH_2 system[33] where the bonding is held mainly between the s and p metal orbitals and the s orbitals of the H atoms. In view of the similarities in the molecular bonding for the different steps of the addition of H_2 on different transition metal atom centers, it is not surprising that they also show similarities on their mechanisms of dissociation of the H–H bond. So the origin of this dissociative mechanism can be simplified and viewed as two simultaneous charge-transfer processes (Figure 2), that is, the charge donation from the σ orbital of the H_2 to the metallic atomic center and the back donation from this center (mainly through the d_{yz} orbital) to the antibonding σ^* of H_2. Both processes have as a final consequence the weakening or even the breaking of the H–H bond.

In view of the efficient photoinduced reductive elimination process

$$H\text{–}M\text{–}H + h\nu \rightarrow M + H_2$$

observed in other transition metal dihydride complexes,[34,35] we investigated the nature of the first unoccupied molecular orbitals for the bent equilibrium configuration of our CuH_2 molecular complex in order to learn some details about this photocatalytic behavior. A detailed analysis of the first three unoccupied orbitals and the partially occupied HOMO orbital (Table IV) reveals that they have an antibonding or nonbonding character with regard to the copper–hydrogen bonds but bonding character with respect to the hydrogen σ bond (with the exception of the $2b_2$ orbital where the σ^* H_2 orbital is present). Such is the case for the $4a_1$, $5a_1$, and $2b_1$ orbital which have pure p character. A photoexcitation of the CuH_2 molecular complex, for example, to the $4a_1$ or $5a_1$ electronic level, would be effective enough to promote the mentioned photoreductive elimination reaction.

IV. Outlook and Perspectives

Before trying to derive conclusions from our present results, we ought to compare the potential energy curves for the H_2–copper surface given in the literature.[27] We already noted that our comparison is necessarily limited to the type C sites which are denoted with the number 1 in Table IV of ref 27. Our value for the activation energy of H_2 lies between their extreme values (18–48 kcal/mol) and is close to their average value of ~32 kcal/mol. Furthermore, we can see that our prediction[16] that the Cu + 2H limit lies well above the energy for the Cu + H_2 reactants is also in agreement with the original molecular beam studies.[28] In effect in Figure 19 of ref 28 this is clearly depicted in a one-dimensional diagram of the interaction of hydrogen with the copper surface for type C sites. Consequently we consider our present results in reasonable agreement with previous results,[26-28] and we shall now try to correlate our results with catalytic data.

For oxidative addition and reductive elimination of H_2 on copper we see that the dissociative adsorption is predicted correctly in our calculations only if the important interactions between the ground and excited states of Cu atoms are taken into account. By itself the lowest state would imply an unfavorable barrier of 66 kcal/mol, but through the long-established but far from commonly mentioned mechanism of the Herzberg–Teller coupling with the excited states of Cu, the barrier goes down to a reasonable value of 28.6 kcal/mol which is close to the experimental heat of dissociative adsorption.[19] A similar barrier, of course, would have to be surmounted (~20–22 kcal/mol) for the exothermic reductive elimination of H_2 from this active center. Thus we see how, albeit in an indirect fashion, the influence of the excited states is decisive in the evolution of the relevant quantities of the metal atom–adsorbate molecular interactions that are so important in the theoretical efforts to understand catalytic phenomena.

A more direct participation of the excited states exists in processes such as the photochemical Cu* + H_2 reaction discussed in ref 15 and 16. Only the participation of an excited state Cu(^{2}P) could possibly trigger the reaction which thenceforth could start indistinctly (via nonradiative transitions) from the Cu(^{2}D) or Cu(^{2}S) states. This leads us to the following questions: to what point does the addition of ligands of different nature to a metal atom in a homogeneous catalyst or perhaps the addition of a cocatalyst or so-called promoter induce a greater participation of the transition metal atom excited states and through this participation induce the dramatic changes that are observed in catalytic activity?

For the present case of the oxidative addition and reductive elimination of H_2 on a metal atomic center, these questions seem to have a direct answer. For example, the different chemical activities of Ni and Pd atoms toward the oxidative addition of H_2 can be understood from their differences in electronic structures. As it has been pointed out,[32a] the lowest singlet state of a Ni atom has a d^9s^1 electronic structure, which is perfectly suited for forming the two bonds with the hydrogens, whereas the lowest state for the Pd atom has a d^{10} electronic structure which can form only a van der Waals complex with the H_2 molecule. This

electronic state of the Pd atom is, however, 22 kcal/mol lower in energy than its d^9s^1 electronic state, and therefore it must form bonds with a bond energy of at least 22 kcal/mol to be stable. When two H_2O ligands are added to the Pd atom, this last electronic situation is induced.[32] In fact, the population analysis shows a tendency to depopulate the d orbitals, and it is speculated[32a] that with other ligands like CO or Ph_3, which are better electron acceptors, this depopulation should increase and therefore facilitate the oxidative addition of H_2 on a Pd atomic center with this more appropriate d^9s^1 electronic structure.

An analogous situation is found in our present results, that is, the tendency of the Cu atom to have a d^9s^2 electronic structure in order to be able to capture the H_2 molecule (see Table II). Naturally this electronic structure is facilitated by the presence of the electronic excited states of the Cu atom. We can notice as in the case of $Pd(H_2O)_2$ system that this electronic structure would be also induced by the presence of a ligand. In fact, if we consider in a speculative way the HCuH system as a metal complex model where H_2 addition can occur, then we do not need to resort to the photoexcitation of the Cu atom in order to give forth the pathway for the appropriate transformation of the electronic structure because now the HCuH complex has such structure. One more example of the correlation between the electronic excited states of a metal atomic center and the ligand effects toward its catalytic activity is found for NiH_2, CoH_2, and FeH_2.[32,33] In these cases the oxidative addition and the reductive elimination are feasible only when the excited states—^1D (d^9s^1), ^2F (d^8s^1), and ^3F (d^7s^2) of Ni, Co, and Fe, respectively—are considered, and the excited states is likewise the probable state for the conformations of L_nMH_2 complexes with M = Ni, Co, Fe.[32b,33]

To our knowledge, no previous studies have been carried out about the role played by the transition metal atom's excited states on a complete catalytic process. In fact, very few ab initio studies of a catalytic process itself, let alone the question of the excited states, have ever been attempted.[41-43] Also such studies were by necessity of relative modest computational sophistication, remaining at the SCF level. This is the case, for instance, of the studies[43] on titanium-aluminum catalytic complexes for Ziegler-Natta polymerization. From the theoretical results of ref 43 we now make some intriguing speculations about the possible participation of the excited states of the Ti atom. At least in ref 43 one thing was clearly established: that from the initiation of the reaction, (the entrance of the ethylene into the titanium coordination sphere), the aluminum atom, namely the cocatalyst, started to interact indirectly with the olefin. In that study the narrowing of the HOMO-LUMO gap and the constant changes in the s-d participation of the titanium on the highest occupied orbital throughout the process apparently hint at such participation of the Ti excited states. Therefore, a reexamination of the Ziegler-Natta process, perhaps at the pseudopotential level, in order to cut down the excessive size of the all-electron calculations,[43] but including configuration interaction, may be able to establish the role of the Ti excited states, and this appears to be quite attractive.

Acknowledgment. We express our gratitude to Dr. E. Poulain for all his worthy comments and effective help in some of the present calculations as well as his computational assistance, to our colleagues at the Laboratoire de Physique Quantique of Toulouse University for providing us with the CIPSI programs, and especially to Drs. Jean-Pierre Daudey and J. C. Barthelat. This research was partially supported by CONACYT, PVT/EN/NAL/81/1557.

Registry No. H_2, 1333-74-0; Cu, 7440-50-8.

(41) Dedieu, A. *Inorg. Chem.* **1980**, *19*, 375.
(42) Daudey, J. P.; Jeung, G.; Ruiz, M. E.; Novaro, O. *Mol. Phys.* **1982**, *46*, 67.
(43) Novaro, O.; Blaisten, E.; Clementi, E.; Giunchi, G.; Ruiz, M. E. *J. Chem. Phys.* **1978**, *68*, 2337.

Clay Modified Electrodes. 3. Electrochemical and Electron Spin Resonance Studies of Montmorillonite Layers

Deniz Ege, Pushpito K. Ghosh, James R. White, Jean-Francois Equey, and Allen J. Bard*

Contribution from the Department of Chemistry, The University of Texas at Austin, Austin, Texas 78712. *Received December 7, 1984*

Abstract: Films (about 30 nm to 3μm thick) of the clay mortmorillonite, with and without added poly(vinyl alcohol) (PVA), were cast on conductive substrates (SnO_2/glass, glassy carbon, platinum) and used as electrodes. Electron spin resonance of the incorporated probe, tempamine, and X-ray diffraction measurements showed that the films with clay alone were oriented, while those containing PVA were random and swollen. The electrochemistry of cationic species incorporated into the films, e.g., $Ru(bpy)_3^{2+}$, $Os(bpy)_3^{2+}$, $Fe(bpy)_3^{2+}$, is described; the effective diffusion coefficients of the Os and Fe species in these films were $\sim 10^{-12}$ cm^2 s^{-1}. Neutral (hydroquinone) and several anionic species, while not incorporated into the film, can diffuse through it to the substrate. Chronoamperometric and rotating disk electrode measurements were employed to study this diffusion. Catalytic hydrogen production at a clay/Pt/PVA film containing propyl viologen sulfonate was found.

The modification of electrode surfaces by coverage with a thin layer of a treated clay was recently reported from this laboratory.[1] Cationic species, e.g., $Ru(bpy)_3^{2+}$ (bpy = 2,2′-bipyridine), $Fe(bpy)_3^{2+}$, MV^{2+} (methyl viologen), could be incorporated into sodium montmorillonite films; for thicker films (ca. 3 μm) clay premixed with poly(vinyl alcohol) (PVA), with or without colloidal platinum, produced more durable films that more readily incorporated electroactive ions.[1] In a separate communication, clay films were shown to be potentially useful as supports for finely dispersed metals and metal oxides which can function as catalysts.[2] For example, ruthenium dioxide incorporated into the clay films promotes the oxidation of water in the presence of electrochemically produced $Ru^{III}(bpy)_2[bpy\text{-}(CO_2)_2]^+$ with regeneration of

(1) Ghosh, P. K.; Bard, A. J. *J. Am. Chem. Soc.* **1983**, *105*, 5691-5693.
(2) Ghosh, P. K.; Mau, A. W.-H.; Bard, A. J. *J. Electroanal. Chem.* **1984**, *169*, 315-317.

0002-7863/85/1507-5644$01.50/0 © 1985 American Chemical Society